

Arrays of Microcavity Plasma Devices: Versatile Platform for The Next Generation of Plasma Displays

J. G. Eden and S.-J. Park
 Laboratory for Optical Physics and Engineering
 University of Illinois, Urbana, IL, USA
 Phone: 217-333-4157, E-mail: jgeden@uiuc.edu

Abstract

Microcavity plasma devices having characteristic dimensions below 100 μm have been investigated as a candidate for the next generation of plasma displays. Arrays of inverted pyramid microcavity devices, fabricated in Si with emitting apertures of $(50 \mu\text{m})^2$ and designed for AC or bipolar excitation, demonstrate a luminous efficacy above 6 lm/W at pressures up to and beyond one atmosphere of Ne/Xe mixtures. Also the design of analogous microplasma devices in ceramic multilayer structures or plastic substrates is discussed.

1. Introduction

Improving the luminous efficacy, pixel resolution, and reducing the cost of the PDP fabrication are the most important challenges to strengthening the competitive position of this display technology in consumer markets. Current efforts are pursuing this goal along several lines, including redesign of the cell structure, and increasing the Xe content.

Microcavity plasma devices are characterized by the spatial confinement of a nonequilibrium plasma to a microcavity with a characteristic cross-sectional dimension of nominally 10-100 μm , nanoliter volumes, and the production of stable, glow discharges at gas pressures up to and beyond one atmosphere [1-2]. Since several microcavity devices have a vertically oriented electrode system, the device structure can be altered simply by a modification of multilayer components without loss of spatial resolution. Conventional mass production techniques can be used to fabricate arrays of microplasma devices having precisely-controlled microcavity dimensions and dielectric structures, thereby tailoring the electric field within the microcavity.

Furthermore, there are no barriers to the realization of arrays of considerably greater active area through the implementation of conventional

process technology. Recent results from our laboratory are reported here, in which the luminous efficacy, spatial resolution and electrical characteristics of microcavity arrays have been investigated.

2. Silicon Microcavity Plasma Devices

Since the basic design of microplasma devices having an inverted square pyramidal microcavity was introduced in 2001, the development of device structure has focused on the reduction of the plasma volume (nano- or picoliters), ac operation, improved lifetime, and enhanced luminous efficacy. An inverted square pyramid microcavity with an emitting aperture (pyramid base dimensions) of $50 \times 50 \mu\text{m}^2$ and Si(111) sidewalls is produced by anisotropic, wet chemical etching of Si(100). The detailed structure of the device is shown in Fig. 1. Note that MgO is not presently incorporated into these devices but our expectation is that doing so will further improve performance. Image (a) of Fig. 2 is a scanning electron micrograph (SEM) of a single $50 \times 50 \mu\text{m}^2$ microcavity plasma device and the right half of the figure (2(b)) shows a portion of an array in which the device pitch is 100 μm and, therefore, the array

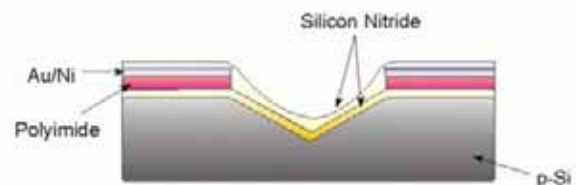


Fig. 1. Diagram (not to scale) of the cross-section of an inverted square pyramid microcavity plasma device, fabricated in Si. The dimensions of the pyramid at its base (i.e., emitting aperture of the microcavity) are $50 \times 50 \mu\text{m}^2$ for the devices discussed here.

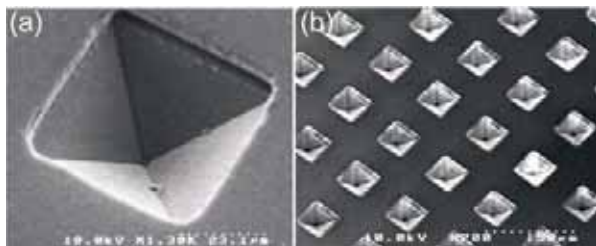


Fig. 2. Scanning electron micrographs (SEMs) of: (a) a single inverted-pyramid microcavity plasma device with base dimensions (emitting aperture) of $50 \times 50 \mu\text{m}^2$, and (b) a portion of an array of microplasma devices in which the device pitch is $100 \mu\text{m}$.

filling factor is 25%. Arrays as large as 250,000 devices with active areas of 25 cm^2 have been fabricated and tested to date. One signature of this device structure is the extraordinary uniformity of the emission from device-to-device. Analysis of digital images of the spatially-resolved fluorescence from 200×200 and 500×500 arrays shows that the peak emission intensity is uniform from device-to-device, across the entire array, to within $\pm 10\%$. To measure luminous efficacy, a commercial green phosphor ($\text{Mn}:\text{Zn}_2\text{SiO}_4$) was screen-printed onto a glass plate (1 mm in thickness) which was mounted $\sim 2 \text{ mm}$ above the array. The array operated with Ne/50% Xe gas mixtures. The luminous efficacy of a 500×500 array of $(50 \mu\text{m})^2$ rises rapidly with p_{total} (and, hence, the Xe partial pressure) as a consequence of the increasing formation efficiency of the Xe_2 excimer. Values above 6 lumens/W are observed for total pressures of 700 and 800 Torr.)[3]. These results, as well as similar measurements for Ne/Xe mixtures with reduced Xe content (5-30%), suggest that further increases in efficacy can be expected by raising the Xe content beyond 50%.

Also, as noted earlier, the incorporation of MgO into the array structure is likely to reduce significantly the required voltages. It is clear that increasing the luminous efficacy of the array by raising p_{total} from 500 to 800 Torr exacts only a small penalty in voltage which is more than offset by the increased radiative efficiency as well as an obvious benefit afforded by atmospheric pressure operation—eliminating the pressure differential across the vacuum packaging of the array. We have fabricated several different types of arrays designed for addressability, and have adopted a vertically aligned three-electrode system. Accordingly, the device structure can be altered

simply by modification of the multilayer components without the loss of spatial resolution. With conventional photolithographic and thin film processing techniques, we have fabricated metallic patterns which can be utilized as addressing and sustain electrodes. Figures 3 shows an example of the independently addressable microcavity arrays and operation of the array in Ne, respectively.

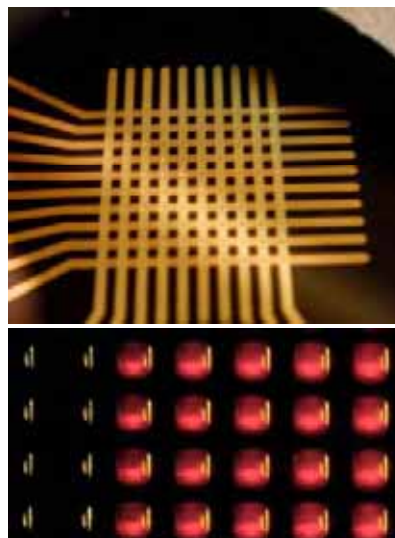


Fig. 3. Photographs of a prototype microcavity array having independently addressable 10×10 pixels (top), and a magnified view of a portion of an array of addressable Si devices showing selective operation of the devices (bottom).

3. Ceramic Device

We have fabricated and successfully demonstrated stable operation of monolithic ceramic arrays having $100\text{--}200\mu\text{m}$ diameter cavities. Prepared by commercial screen-printing or simple green-tape casting methods, all of the discharge components can be incorporated in a single body chip and there are no barriers to scaling array area. Furthermore, robust fired ceramics promise longer operational lifetime. Having a total thickness of $650 \mu\text{m}$, the array is driven by multiple addressable electrodes formed inside the ceramic chip. Also, $200 \mu\text{m}$ thick silver electrodes are encapsulated inside the LTCC dielectrics which have a dielectric constant of 40. As shown in Figure 4, each linear array consists of 72 microcavities powered by two coplanar electrodes having a fixed spacing of $220 \mu\text{m}$.

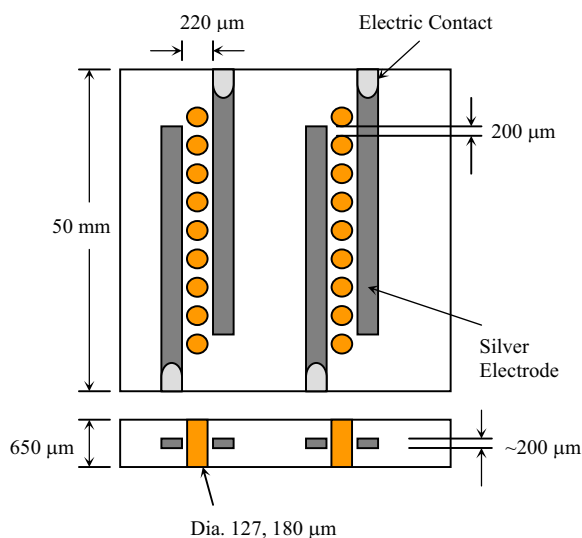


Fig. 4. Schematic diagrams of top and end-on views of linear arrays of ceramic microcavity devices.

Two different devices with cavity diameters of 127 and 180 μm have been tested to date. As the distance between the silver electrodes is fixed, the dielectric thickness between each electrode and the gas filled discharge cavity is ~ 47 and 20 μm respectively. A 20 kHz bipolar pulsed DC waveform (10 μsec width) pulse provided excitation for the array. Due to the thinner dielectric, the 180 μm device has firing and operational voltages ~ 20 V lower than that required for the 127 μm device. Also, the device current was less than 50 % of 127 μm device. It was found that the phosphor emission intensity increased by a factor 5-9, without a significant change of power consumption when the Xe content is increased from 5 to 15% (with a Ne/Xe mixture). Interestingly, we observed that the operational voltage does not change significantly with increasing Xe content which is unusual for planar PDP discharge systems. These devices show high contrast and excellent uniformity with phosphor layer.

4. Al/Al₂O₃ Multilayer Devices

A group of robust microcavity plasma devices has been fabricated in Al/Al₂O₃ multilayer structures by drawing upon wet chemical processing to grow thin films of nanostructured Al₂O₃ directly from the Al substrate [4]. The chemical and optical properties of Al₂O₃, in combination with an overall device (pre-sealed) thickness of ~ 200 μm , make this a rugged structure that is light and economical and yet able to

withstand high power loadings. Figure 5 is a schematic diagram of a single Al/Al₂O₃ device in cross-section. Nanoporous Al₂O₃ films 5-40 μm in thickness are grown on 127 μm thick Al foil by a multistage anodization sequence. A masking technique allows for 5-20 μm thick dielectric films to be grown on the interior wall of the microcavities and 20-40 μm thick on the Al foil surface, thereby ensuring the formation of plasma within the microcavity and the absence of electrical breakdown elsewhere. The device structure of Fig. 5, comprises two conjoined cylindrical cavities with diameters of 100 μm and 200 μm .

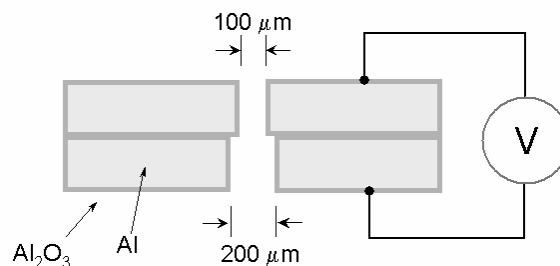


Fig. 5. Cross-sectional diagram (not to scale) of a basic Al/Al₂O₃ microplasma device structure with two conjoined cylindrical cavities.

5. Plastic Devices fabricated by Replica Molding

In this paper, a replica molding method is introduced as a new opportunity for microdischarge device fabrication. Since the technology is based on the molding of polymeric resin, we can increase the scale toward large area discharge arrays inexpensively. Also this approach is capable of fabricating high aspect-ratio cavities with lateral pixel dimensions as small as 1 μm . Similar to other thin plastics, these structures can be fully transparent, light or mechanically flexible.

The microcavity device is fabricated by the stamping of a "master" silicon wafer in a single process, and the master wafer may be used thousands of times to produce cavities without wear. Each replica is produced with high accuracy and repeatability by conventional photolithographic techniques. Because most of the materials used are optically transparent, it will be possible to guide light laterally into and out of the plasma discharge region, so the plasma discharge may be integrated with

optical waveguides. Fig.6 shows one demonstration of a fully transparent and vacuum sealed 20×20 replica molded array having $200 \mu\text{m}$ dia. microcavities, As each microcavity is connected to adjoining emitters by gas feeding line of small cross-section, we can modify the discharge performance selectively.

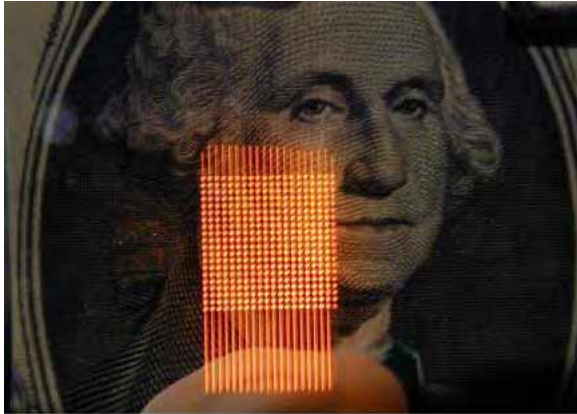


Fig.6. Photograph of 20×20 replica molded array operated in 700 Torr Ne. A dollar bill was placed behind the device to show transparency.

6. Impact

The performance of $50\text{--}200 \mu\text{m}$ scale microcavity devices provides inspiration for the next generation of high resolution plasma display. Spatially confined microdischarges in different platforms such as Si, ceramics and plastics, provide higher pixel-to-pixel contrast, atmospheric pressure operation, and increased luminous efficiencies at higher Xe content. Also, future efforts to optimize device addressability and the firing voltage will undoubtedly yield further improvements in device and array performance. It is clear that the flexibility of these arrays, in combination with the low cost of fabricating radiating structures of large area, suggests the potential utility of this microcavity plasma device design to several applications.

7. Acknowledgements

The support of this work by the Samsung SDI and U.S. Air Force Office of Scientific Research under grant no. F49620-03-1-0391 is gratefully acknowledged.

8. References

- [1] S.-J. Park, J. Chen, C. J. Wagner, N. P. Ostrom, C. Liu, and J. G. Eden, IEEE J. Sel. Topics Quantum Electron., vol. 8, pp. 387-394 (2002).
- [2] J. G. Eden, S.-J. Park, N. P. Ostrom, and K.-F. Chen, J. Phys. D, vol. 38, 1644 (2005).
- [3] K.-F. Chen, N. P. Ostrom, S.-J. Park, and J. G. Eden, Appl. Phys. Lett., 88, 061121 (2006).
- [4] S.-J. Park, K.S. Kim and J.G. Eden, Appl. Phys. Lett., 86, 221501 (2005).